ECS Transactions, 66 (6) 27-38 (2015)
10.1149/06606.0027ecst ©The Electrochemical Society

Fabrication and Characterization of Silicon Microwire Anodes by Electrochemical Etching Techniques

Sandra Nöhren,[a] Enrique Quiroga-González,[b] Jürgen Carstensen,[a] Helmut Föll[a]*

[a] Institute for Materials Science, Christian-Albrechts-University of Kiel. 24143 Kiel, Germany.
[b] Institute for Physics, Benemérita Universidad Autónoma de Puebla (BUAP). 72570 Puebla, Mexico.

With a technique principally allowing for large scale production based on electrochemical etching, silicon microwires for Li ion battery anodes are produced. Silicon wires exhibit high cycling stability with high amount of active material which does not degenerate over the cycling period due to the formation of a homogeneous solid electrolyte interface around each wire. This study summarizes the importance of the (exact) battery work parameters and shows the influence of different wire dimensions on the battery performance and cycling stability. Furthermore, it compares two anode variations in which the wires can be incorporated. FFT-impedance analysis shows the characteristic resistance changes under specific conditions, which relate directly to the processes in the wires during operation, what helps for their optimization.

Introduction

Among different anode materials, nano- or microstructured Si have become increasingly important in recent years. Compared to graphite anodes, Si anodes posess a more than tenfold gravimetric capacity of 4200 mAh/g [1 - 3]. This capacity can be stable over hundreds of cycles if Si is in the form of nano- or microwires. Large cracks form in bulk silicon due to large volume expansions during cycling, leading to open circuits in batteries in a few cycles. Different techniques like standard vapor-liquid-solid (VLS) [4] and metal assisted electroless chemical etching methods (MACE) can be used to structure Si. These techniques are limited by the geometry of the resulting structure of silicon. Randomly distributed pores or wires limit the battery performance because the diffusion of Li into the wires is not homogeneous.

Due to progress in the electrochemical pore formation in n- and p-doped Si by different groups around the world, homogeneous, nano- and micro-structured Si can be produced. With the anodic etching of Si in various electrolytes, different pore structures have been developed [5 - 9]. In this study the electrochemical pore etching process of wire arrays for battery anodes was optimized in order to obtain a silicon wire array with intergrown stabilizing planes. The wire arrays, when used as anodes of batteries, withstand large stresses, and present a stable capacity of 3150 mAh/g for over 100 cycles with an areal capacity of 4.25 mAh/cm^2 [1] a record among Si anode concepts. It is well

known that graphite anodes suffer from a continuously growing solid electrolyte interface (SEI) which forms due to the decomposition of the electrolyte, thus hindering further intercalation of Li in the graphite. Astonishingly for the silicon microwire anodes discussed in this paper we found that the SEI stops to grow after the first three charge/discharge cycles which is one reason for the good cycling stability.

Processing of Si microwires

The formation of Si microwire arrays consist of a series of electrochemical and chemical etching steps. All of these steps need a pre-structuring step by standard photolithography where an array of circles with 1.5 µm in diameter and 3 µm distance is structured on the p-doped (100)-Si wafer. Anisotropic dry and wet (chemical) etching steps allow the formation of inverted pyramids with a depth of around 1 µm with a defined pyramid tip. These inverted pyramids are the starting point for the dissolution of Si during the anodic macropore etching. The electrochemical etching is based on the anodic etching of silicon and can be applied/designed with various electrolytes. Typically, the electrolytes consist of 5 wt. % HF with an addition of an organic solvent like dimethylformamide (DMF). With the addition of water, an oxidation reaction at the pore walls occur. The formed SiO_2 is dissolved by the HF until the oxide is completely dissolved. The process of oxide formation and dissolution is continuous over the etching process [10, 11]. This etching modus allows obtaining wider pores (thinner walls), due to its isotropic nature. Without the addition of water, the oxidation process is limited, and direct dissolution of silicon is performed. Pore modulation is obtained by varying the current density over time, and is enhanced through the addition of polyethylenglycole (PEG), which passivates the pore walls and reduces their over-etching (etching is focused at the pore tips) [4]. By applying a specific current-time profile to the sample, the pores can be modulated according to length and diameter. Figure 1 shows examples of current profiles for obtaining wires with different lengths, with two pore narrowing (obtained by steeply reducing the current). The length can be varied from short pores (36 µm) to longer pores (75 µm) by adapting the etching time and current.

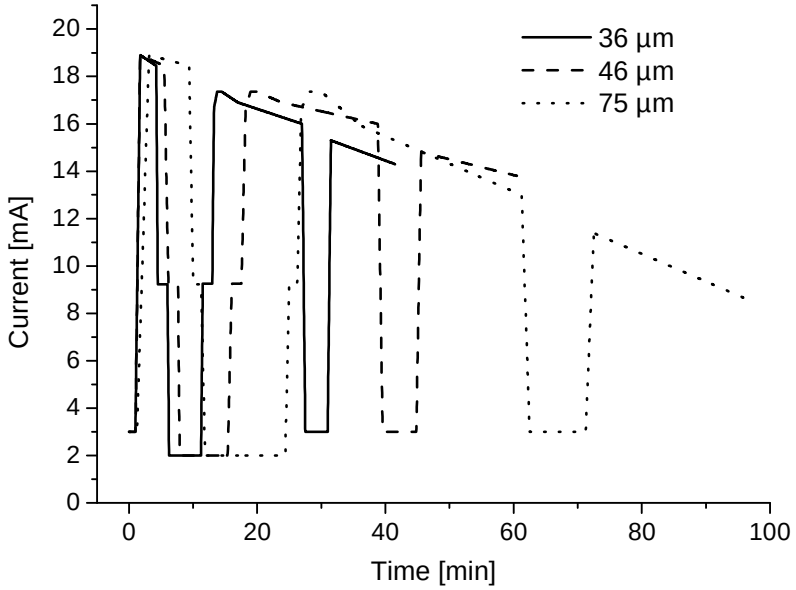

Figure 1: Electrochemical etching profile adapted for various pore lengths, ranging from 36 to 75 µm.

To obtain the wires from macroporous Si purely chemical post etching of the pore walls is used. This chemical etching is performed with an etchant with a low concentration of KOH [1, 4]. The longer the etching is performed, the thinner the wires. The limit of the wire thickness is around 900 nm, when the stabilizing supports are etched away and the wires start collapsing. The combination of both, the electrochemical and chemical etching steps allows the production of wires with various lengths and thicknesses. The process is also scalable to obtain wire arrays over different areas. The sample area can be varied by modulating the etching current and the temperature [12].

Production of battery anodes with the Si microwires

Paste anodes

In order to test lithiation/delithiation as a function of wire thickness a simple paste electrode was fabricated: This approach does not need individual optimization especially for the galvanic embedding of the Si wires into a Cu current collector. For the production of paste anodes, the Si microwires are scratched from the bulk Si substrate and mixed with conductive carbon black (1:1 ratio) and CMC and water. A thin layer of mixed Si wires is casted on top of a Cu foil, and the produced samples are dried in vacuum at 75 °C for 7 h. These paste electrodes are used to facilitate the characterization of the wires themselves when lithiated or delithiated in half cells. The half cells are prepared with metallic Li as counter electrode and with standard battery electrolyte LP 30. LP 30 is the standard battery electrolyte provided by BASF which contains an equal amount of ethylencarbonate (EC) and dimethylcarbonate (DMC) with $LiPF_6$ as Li salt. Figure 2a shows an example of SEM micrograph of a paste electrode. Each wire is surrounded by carbon black, representing conductive paths from the current collector to the Si wires.

To investigate the impact of the thickness and length of the wires on their electrochemical and structural behavior during cycling, wires with five different

thicknesses and five different lengths were fabricated for this study (thicknesses ranging from 1.8 to 1.2 µm with a fixed length of 60 µm, and different length from 36 to 75 µm at a thickness of 1.4 µm). The scale-invariant etching technique makes this definite size modulation possible.

Anodes of wire arrays

While the paste electrodes need the conductive additive carbon black to increase the conductivity, the wire arrays benefit of their high amount of active material without any carbon due to their mechanical integration and stability to the Cu layer. After the electrochemical deposition of the current collector, it is possible to detach the whole array from the substrate. A deliberate change in the current-time profile at the pore tips during the electrochemical etching allows the easy detachment from the substrate [1]. This concept of Si anode is the one used for testing the performance of Si wires in batteries. It is one of the most promising concepts.

a. b.

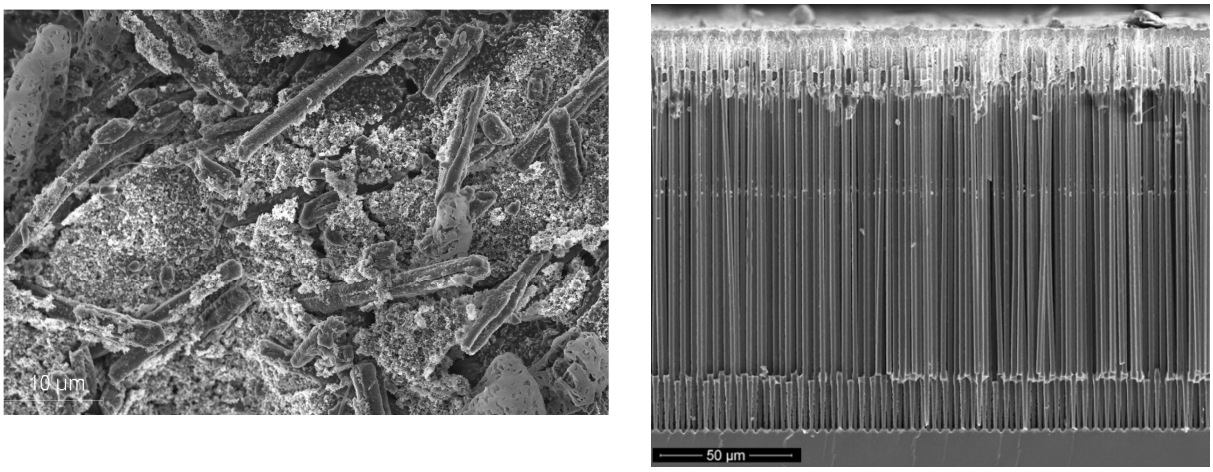

Figure 2: Examples of SEM micrographs of Si microwire anodess a) microwires embedded in a conducting matrix as paste anodes, b) Si wire array with a current collector deposited at its top.

In order to obtain battery anodes, a current collector has to be deposited. In comparison to chemical or physical vapor deposition steps where the adhesion between metal and Si as well as the thickness of the metallic layer has to be improved, the current collector is also deposited purely galvanically. In a first step, a several nm thin Cu seed layer is deposited on top of the Si wires by dissolving Si and reducing the Cu ions. The thickness of the resulting Cu layer after the galvanic deposition is around 50 µm. There is Cu deposition also between the interstices of the wires, enabling a good mechanical contact. The wire tips of 5 to 10 µm are fixed in this Cu layer. Experiments showed that this mechanical integration of the wires into the current collector is a key parameter of the good cyclability. During cycling, the wires expand when Li-ions incorporate into the wires, leaving the fixed part of the silicon “uncharged” – there is no alloy formation in the bottom part of the wires.

Not only the electrochemical and/or chemical etching steps are scale invariant, but also the deposition of the current collector is no longer limited to small areas. To overcome large potential differences across larger areas of the Si wafer (during

deposition), small nucleation centers of Cu are created which are embedded in a polymer matrix (EP 14 184 103.1). Around those nucleation points, the Cu grows homogeneously until the nuclei agglomerate and form a homogeneous Cu layer. The polymer matrix can be doped with additional chemistry previously used in the seed layer deposition which makes this separate step unnecessary. The time for the Cu deposition can be reduced in this step up to 50 % (5 hours).

Electrochemical characterization

The Si wires are characterized by cyclic voltammetry. Additionally in situ FFT-impedance spectroscopy has been used to characterize the anodes. This technique is very powerful, allowing the investigation/distinction of the resistances and capacitances between the electrolyte, SEI and the interface between the SEI and the Si wires. Cyclic voltammetry is used in this work to investigate the potential dependency on the thickness and length of the wires. During voltammetry measurements a (potential) scan is applied reversibly between 1 V and 20 mV for five cycles. Phase transformations can be identified in the form of peaks in the voltammograms. The phase transformations are step-wise lithiation and delithiation of Si with Li-ions, which depend on external and internal parameters during a voltammogram [13, 14]. Figure 3 shows in a comparison typical voltammograms of Si wires with two wire lengths and two thicknesses. The shape of the voltammogram is typical for Si anodes and varies only in the peak positions [13, 15 - 17].

a. b.

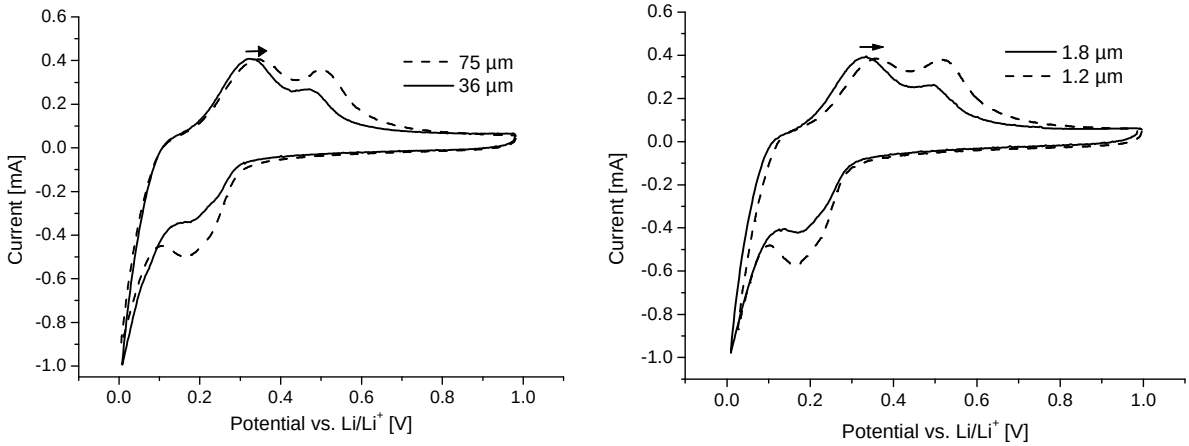

Figure 3: Typical voltammograms for different wire geometries, embedded in paste anodes: a) comparison between two lengths, b) comparison between two thicknesses.

The peaks represent phase transformations and are fully reversible indicated by two peaks during the lithiation (from 1 V to 20 mV) and delithiation (from 20 mV to 1 V, reversal of the potential scan). Li ions are incorporated into the silicon wires in a two-step process forming Li_xSi_y alloys undergoing structural (phase) transformations from crystalline to amorphous upon cycling. A fully lithiation peak, represented in Figure 3a and b, is at the potential where the Li-ions are fully incorporated and Li_xSi_y alloys are formed. If the Li-ions are removed from the anode completely, the fully delithiation peak is formed. The partial lithiation as well as delithiation peaks are formed in between the

conversion from (crystalline) silicon to alloy formation and vice versa. The peak shifts with the size variation are illustrated in Figures 3a and b. The peak shift (here only displayed in detail for the partial delithiation peak) is seen in every peak. The lithiation voltage increases almost linearly with the wire length indicating the longer paths for the Li ions or the electrons. The peak shift in the lithiation voltage can be explained by different numbers of series resistances inside the wires of different length. If the wires are longer, the number of series resistances is increased and the average resistance is larger. Therefore, the increase in the lithiation voltage for longer wires corresponds to higher average resistances inside the wires [13]. Figure 3b indicates the impact of different thicknesses. A comparison between the peak maxima for different thicknesses indicate smaller lithiation and delithiation voltages for thick wires. The average resistance varies with the cross section of the wires which is consequently smaller with thin wires.

Additionally FFT-impedance analysis was performed over three cycles on thick wires (1.8 µm). Figure 4 shows the comparison between the three resistances computed from the measurements, and the recorded current. The electrochemical processes can be modeled with three RC circuits in series. The simultaneous application of DC and AC signals allows to model fast and slow processes on the same sample at the same time. By combining cyclic voltammetry and FFT-impedance spectroscopy, not only the interaction between the paste electrode ingredients can be modelled and the correlation between the formation of the SEI around the wires can be understood as well.

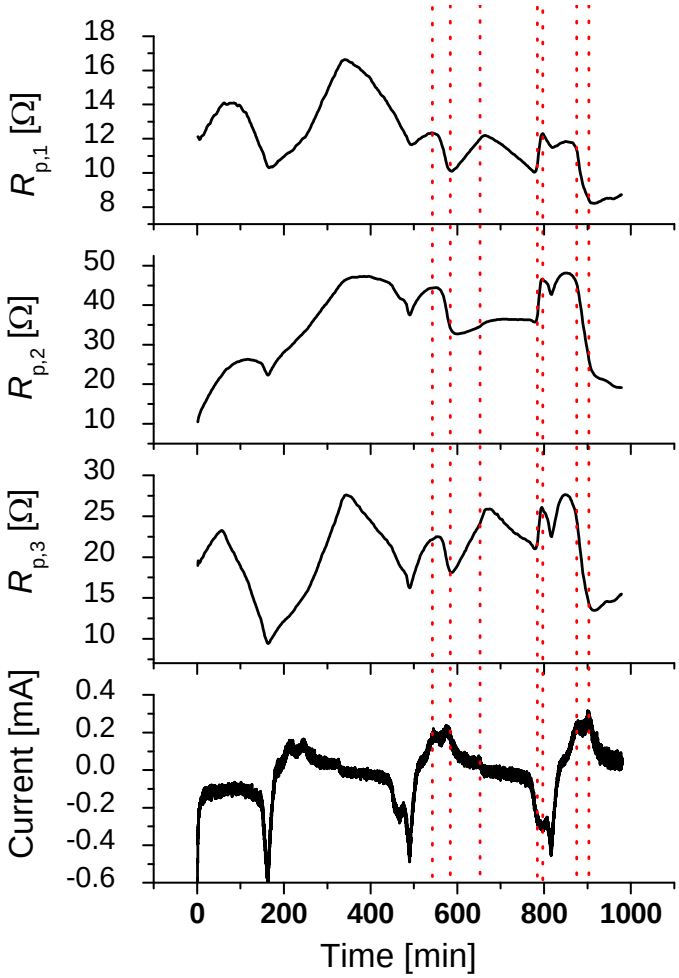

Figure 4: Resistances from FFT-impedance analysis for a wire thickness of 1.8 µm, embedded in paste anodes.

Figure 4 indicates the different behavior of the resistances. $R_{p,1}$ is in the same order of magnitude as the other resistances but slightly smaller while the other two resistances are similar in their values. By comparing the behavior of $R_{p,1}$ on the time scale, the values change in the first cycle while the change of behavior stabilizes in the continuing cycles (almost constant in the last cycles – not presented in this work). This resistance may be related to the SEI [18 - 20], which forms during the first cycles. Previous to the cycling process, there exists a large potential barrier between the electrolyte and the Si wires, since the interface is abrupt. After the first cycles, this interface gets smoother through the formation of SEI, which contains Si and decomposition products of the electrolyte [21 - 24]. In the case of Si microwires, using appropriate cycling voltage limits, the SEI stabilizes after the first couple of cycles [25]. $R_{p,1}$ is nearly independent of the lithiation/delithiation state (figure 4), and its behavior is only different during the formation or decomposition of the electrolyte.

$R_{p,2}$ on the other hand exhibits the highest value during the cycling. This behavior can be directly correlated to the charge transfer into the silicon wires. Obviously for thicker wires the resistance increases which is in good accordance to the more active material which has to be penetrated and the more bonds which have to be broken when Li ions diffuse into the Si wires. Figure 5 compares two resistances and two diffusional processes happening inside paste electrodes. Corresponding to figure 3b, both wire thicknesses are

displayed here. Direct comparison indicates the complementary behavior between both the capacitances and resistances. While $R_{p,1}$ decreases over time, $R_{p,3}$ increases over time (see Figure 5b). On the other hand, the capacitances vary about two orders of magnitude. Due to the direct correlation between the area and the capacitance, thick wires may have a reduced surface to volume ratio (smaller interface to the electrolyte) and show smaller capacitance in comparison to thin wires. Nevertheless, $R_{p,3}$ can most probably be correlated to the (elastic) interaction between the wires and the surrounding matrix containing carbon black. During the large volume expansion, the wires breathe, contracting the conducting material around the wires and producing voids. With longer cycling time, the voids around the wires need longer time to be filled again and the electrolyte has the chance to interact with the paste directly limiting the battery performance.

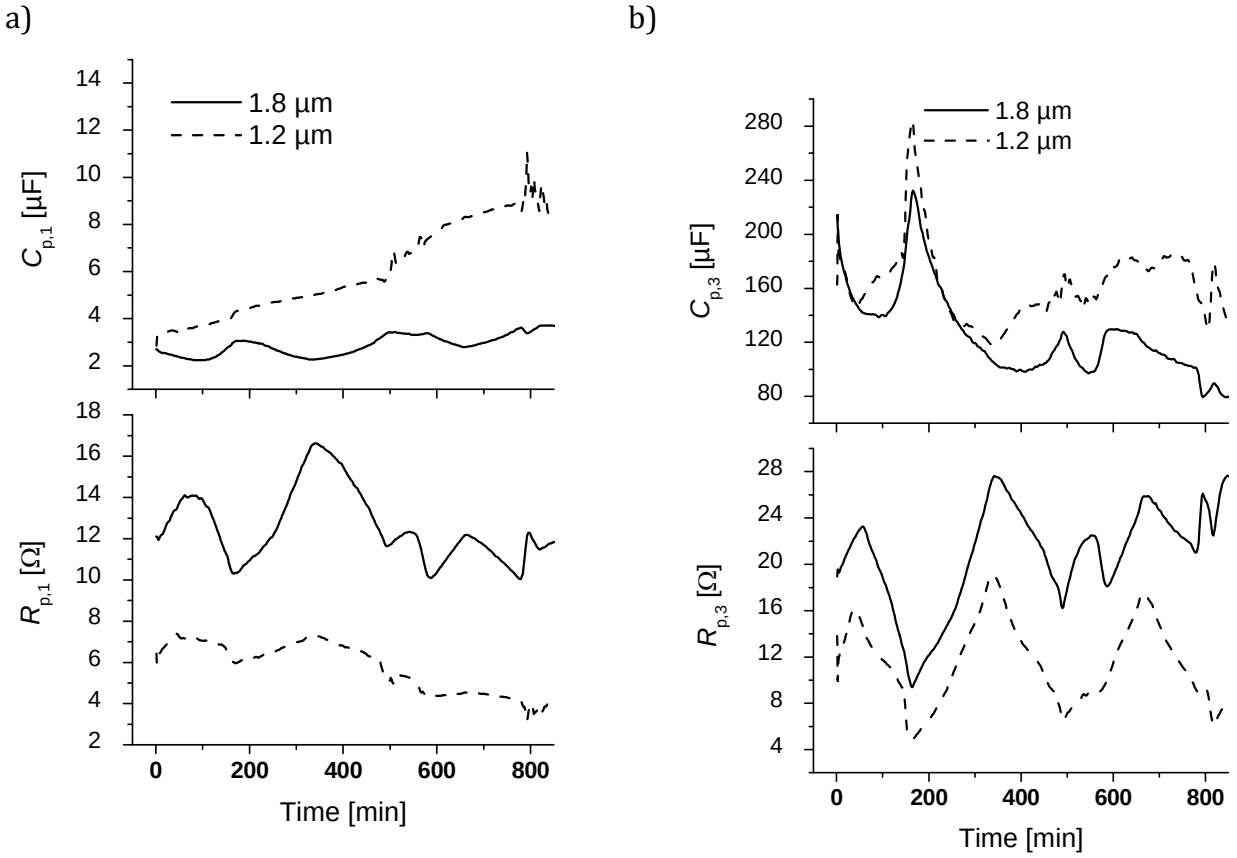

Figure 5: Comparison of resistances for thick wires embedded in paste anodes a) $R_{p,1}$ and $C_{p,1}$ b) $R_{p,3}$ and $C_{p,3}$.

During the breathing of thick wires, less voids or paths for the electrolyte are formed due to the limited space in the matrix leading to the connection from the cyclic voltammograms and the potential dependency. Increasing thickness of the wires, the $R_{p,3}$ increases (consequently, the capacitance decreases) and a second maxima appears (which is more pronounced in thinner wires). At 560 min (compare figures 4 and 5b, indicated with a straight line), the system is between both delithiating peaks (conversion between the partial and fully delithiation peaks – removing Li-ions and conversion from Li_xSi_y alloys into pure Si). During this conversion, larger volume expansion occurs, leading to higher resistances (and higher energy which has to be provided) because of the increase in surface area.

Whereas in paste electrodes the SEI is formed and probably damaged due to its direct contact with the conductive material during the breathing while cycling, in wire arrays the SEI is formed homogeneously from top to the bottom, and is stable over hundreds of cycles. In order to see the difference between the processes inside paste electrodes and wire arrays, FFT-impedance analysis was also performed on wire arrays which allows a direct comparison of the time constants in both the paste anodes as well as in the wires array anodes. Results of the last variant are shown in figure 6. The equivalent circuit are here also three *RC* circuits in series for which three major time constants are modelled and correlated in Figure 6. The slowest time constant τ_3 represents the charge transfer to the Si wires. The other two time constants, whose behavior and order of magnitude are similar, represent the conduction through the electrolyte (τ_1) and through the SEI (τ_2).

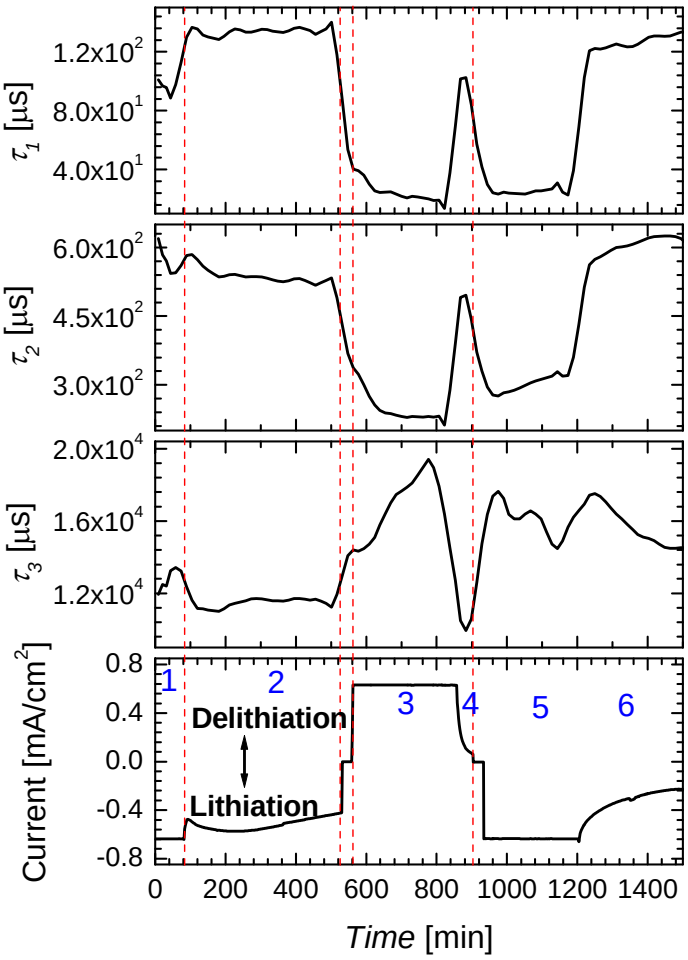

Figure 6: Time constants from FFT-impedance analysis for wire array anode [1].

The maxima in the slowest time constant τ_3 can be directly correlated to the inflection points in the second derivative of the voltammogram. Those inflection points can be correlated to the phase transformations occurring in Si. By directly comparing the two variations and their FFT analysis, the time constants differ about three orders of magnitudes. This behavior can be explained by the way of connecting the wires to the current collector. Paste anodes which are mixed with conducting carbon black provide easier connectivity to the active material which is indicated by the faster time constants (not shown in this study – correlation of capacitances of figures 4,5,6). Nevertheless, due to the interaction between the additives and the Si wires during breathing, the battery

performance is hindered. The volume expansion during lithiation/delithiation processes lead to void formation around the wires (loss of contact to the current collector). For the wire arrays (compare Figure 1b), the wires are fixed from one side to the current collector and can only expand in one direction. Although the time constants are faster in paste anodes, the battery performance could be optimized and the problems can be indicated due to the simultaneous FFT-impedance analysis.

The FFT-impedance spectroscopy is a powerful tool to indicate battery performance processes which can be used to change fabrication processes, leading to higher (battery) efficiencies.

Battery performance

The silicon microwire arrays exhibit under the optimal charging conditions a stable capacity of about 3150 mAh/g over 300 cycles. Studies have shown [1, 25] that a capacity limitation to 75 % of the nominal capacity and a relatively slow cycling rate of *C*/10 are necessary to allow stable SEI formation in the first cycles without any dendrite or crack formation (as happened if cycled to the full capacity). Figure 7a indicates the battery performance under these conditions. After the first four cycles, the cycling rate is increased to *C*/2 [25].

a. b.

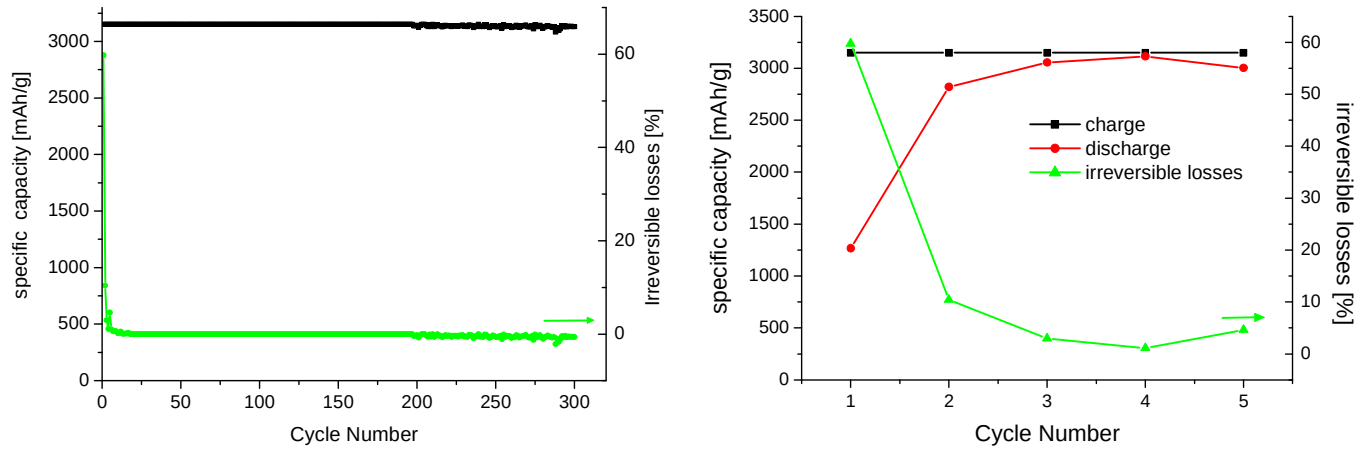

Figure 7: Battery performance with a capacity limitation of 75 % SOC a) for 300 cycles, b) 5 cycles to demonstrate the irreversible losses occurring in the first three cycles.

Figure 7b shows the first charging/discharging cycles. Here, the comparison between the lithiation/delithiation curves and the irreversible losses indicate that the wires only suffer from losses in the first couple of cycles due to the formation of the SEI.

Conclusion

This paper presented a scale invariant production technique of Si microwire arrays which can be used successfully as anodes for Li-ion batteries. Due to the way of fabrication defined thicknesses and lengths can be modelled and characterized in either paste electrodes with the addition of conducting additives or as arrays with the mechanical stability of the current collector. It also showed the unique way of characterizing or combining standard cyclic voltammetry with FFT-impedance

spectroscopy to allow distinct information about the influence of the various geometries to the compound and with it on the battery performance. The potential dependency on the thickness and the length in the paste electrodes could be correlated to the breathing inside the matrix.

Acknowledgments

Special thanks goes to DFG “Elektrochemische und mikrostrukturelle Untersuchung der Prozesse in Anoden für Hochkapazitäts-Lithium-Ionen-Batterien basierend auf Si-Mikrodrahtanordnungen” (Fkz: FO 258/17-1) for their funding of this project.

References

[1] E. Quiroga-González, J. Carstensen, and H. Föll, Materials, 6 (2013) 626.

[2] A. Jossen and W. Weydanz, Moderne Akkumulatoren richtig einsetzen, Reichardt Verlag, Leipheim (2006).

[3] G.A. Nazri and G. Pistoia, Lithium Batteries: Science and Technology, Springer (2009).

[4] E. Quiroga-González, E. Ossei-Wusu, J. Carstensen, and H. Föll, J. Electrochem. Soc., 158(11) (2011) E119.

[5] V. Lehmann, Electrochemistry of Silicon, Wiley-VCH, Weinheim (2002).

[6] H. Föll, M. Leisner, A. Cojocaru, and J. Carstensen, Electrochim. Acta, 55(2) (2009) 327.

[7] R.B. Wehrspohn and J. Schilling, MRS Bulletin, 26(8) (2001) 623.

[8] V. Lehmann and S. Rönnebeck, J. Electrochem. Soc., 146(8) (1999) 2968.

[9] A. Slimani, A. Iratni, H. Henry, M. Plapp, J. Chazalviel, F. Ozanam, and N. Gabouze, Nanoscale Res. Lett., 9 (2014) 585.

[10] J. Carstensen, M. Christophersen, and H. Föll, Mater. Sci. Eng. B, 69-70 (2000) 23.

[11] H. Föll, M. Leisner, A. Cojocaru, and J. Carstensen, Materials, 3 (2010) 3006.

[12] E. Quiroga-González, J. Carstensen, and H. Foell, Nanoscale Res. Lett., 9 (2014) 5.

[13] S. Noehren, E. Quiroga-González, J. Carstensen, and H. Foell, ECS Transactions, x (2015) 9.

[14] M. McDowell, S.W. Lee, W.D. Nix, and Y. Cui, Adv. Mater., 25 (2013) 4966.

[15] K. Kang, H.S. Lee, D.W. Han, G.S. Kim, D. Lee, G. Lee, Y.M. Kang, and M.H. Jo, Appl. Phys. Lett., 96 (2010) 0531101.

[16] M.N. Obrovac and L. Christensen, Electrochem. Solid State Lett., 7(5) (2004) A93.

[17] V.L. Chevrier, H.M. Dahn, and J.R. Dahn, J. Electrochem. Soc., 158(11) (2011) A1207.

[18] J.J. Wu and W.R. Bennett, NASA Technical reports Server (2012) 1.

[19] K. Xu, Chem. Rev., 104 (2004) 4303.

[20] S.S. Zhang, K. Xu, and T.R. Jow, Electrochimica Acta, 51 (2006) 1636.

[21] K.W. Schroder, H. Celio, L.J. Webb, and K.J. Stevenson, J.Phys.Chem.C, 116 (2012) 19737.

[22] U.S. Vogl, S.F. Lux, E.J. Crumlin, Z. Liu, L. Terborg, M. Winter, and R. Kostecki, J.Electrochem.Soc., 162 (2015) A603.

[23] H. Wu, G. Chan, J.W. Choi, I. Ryu, Y. Yao, M.T. McDowell, S.W. Lee, A. Jackson, Y. Yang, L. Hu, and Y. Cui, Nnano, 7 (2012) 6.

[24] W. Xu, S.S.S. Vegunta, and J.C. Flake, J. Power Sources, 196(20) (2011) 8583.

[25] E. Quiroga-González, J. Carstensen, and H. Föll, Electrochim. Acta, 101 (2013) 93.